# Theaflavins inhibit glucose transport across Caco-2 cells through the downregulation of the Ca^<2+>/AMP-activated protein kinase-mediated glucose transporter SGLT1

Li, Baorui
Department of Bioscience and Biotechnology, Faculty of Agriculture, Graduate School of Kyushu University

Fu, Lei
Department of Bioscience and Biotechnology, Faculty of Agriculture, Graduate School of Kyushu University

Abe, Chizumi
Department of Bioscience and Biotechnology, Faculty of Agriculture, Graduate School of Kyushu University

Nectoux, Alexia M.
Department of Bioscience and Biotechnology, Faculty of Agriculture, Graduate School of Kyushu University

他



出版情報：Journal of Functional Foods. 75 (104273), 2020-12. Elsevier
バージョン：

Journal of Functional Foods 75 (2020) 104273

Contents lists available at ScienceDirect

Journal of Functional Foods

journal homepage: www.elsevier.com/locate/jff

# Theaflavins inhibit glucose transport across Caco-2 cells through the downregulation of the $Ca^{2+}$/AMP-activated protein kinase-mediated glucose transporter SGLT1

Baorui Li [a,1], Lei Fu [a,1], Chizumi Abe [a], Alexia M. Nectoux [a], Ayaka Yamamoto [b], Toshiro Matsui [a,*]

[a] Department of Bioscience and Biotechnology, Faculty of Agriculture, Graduate School of Kyushu University, 744 Motooka, Fukuoka 819-0395, Japan
[b] Yaizu Suisankagaku Industry Co., Ltd., 5-8-13 Kogawashinmachi, Yaizu, Shizuoka 425-8570, Japan

ARTICLE INFO

*Keywords:*
Theaflavins
Anti-diabetes
Glucose transport
SGLT1
AMPK

*Chemical compounds studied in this article::*
Theaflavin (PubChem CID: 135403798)
Theaflavin-3′-*O*-gallate (PubChem CID: 71307578)
Theaflavin-3,3′-di-*O*-gallate (PubChem CID: 135536164)

ABSTRACT

The study investigated the effects of theaflavins, which are intestinally non-absorbable compounds, on intestinal glucose transport in Caco-2 cells. $^{13}C_6$-Glucose transport experiments clearly revealed that glucose transport across Caco-2 cells was significantly ($p < 0.01$) inhibited by theaflavins. When Caco-2 cells were treated with 40 μM theaflavins for 24 h, the expression of SGLT1 expression was significantly ($p < 0.05$) suppressed, whereas no difference in GLUT2 expression was observed. The theaflavin-induced inhibition of glucose transport was reversed by the inhibition of influx routes mediated by OATP and MCT transporters. A Wes analysis established that theaflavin-induced phosphorylation of AMPK was significantly ($p < 0.05$) suppressed by the inhibition of endoplasmic reticulum $Ca^{2+}$-release and CaMKK β. These findings demonstrated for the first time that theaflavins can inhibit glucose transport across Caco-2 cell monolayers through the suppression of SGLT1 expression partly via the activation of the intracellular $Ca^{2+}$/CaMKK β/AMPK signaling pathway.

## 1. Introduction

Type II diabetes mellitus (T2DM), caused by deficient insulin secretion or inadequate insulin utilization, has been reached epidemic proportions in developed as well as developing countries (Hu, 2011). Chronic hyperglycemia associated with T2DM leads to glucose toxicity and causes numbers of complications, including macrovascular disorders (coronary artery disease, peripheral arterial disease, and stroke) and microvascular disorders (diabetic nephropathy, neuropathy, and retinopathy) (Wilmot et al., 2012). Hence, the control of postprandial hyperglycemia has been suggested as an alternative approach for preventing or delaying the developments of diabetes or diabetes-related complications.

There is a growing interest in food-derived inhibitors or anti-hyperglycemic functional foods for the management of T2DM, due to their potential for regulating postprandial hyperglycemia. A possible approach is the inhibition of carbohydrate hydrolyzing enzymes, including α-amylase and α-glucosidase in the digestive tract. Natural acylated anthocyanins (Matsui, Ueda, Oki, Terahara, & Matsumoto, 2001), *Cassia auriculate* extract (Sri Lanka) (Abesundara, Matsui, & Matsumoto, 2004), catechins (Matsumoto, Ishigaki, Iwashina, & Hara, 1993), and theaflavins (Matsui et al., 2007), possibly inhibit intestinal maltase activity specifically, as their administration *in vivo* leads to an acute increase in postprandial blood glucose levels (BGL) in maltose-loaded rats. However, the anti-hyperglycemic effect via the inhibition of carbohydrate digestion is restricted by the timing of dietary intake. An alternative strategy in preventing diabetes is therefore, the suppression of glucose absorption during the intestinal transport process (Baldea,

*Abbreviations:* ABC, ATP-binding cassette; AMPK, AMP-dependent kinase; GLUT2, glucose transporter 2; $[Ca^{2+}]_i$, intracellular $Ca^{2+}$ concentration; LC-TOF-MS, liquid chromatography-time-of-flight-mass spectrometry; MALDI-MS, matrix-assisted laser desorption/ionization mass spectrometry; PEPT1, peptide transporter 1; PKC, protein kinase C; PMP, 1-phenyl-3-methyl-5-pyrazolone; SAR, structure-activity relationship; SGLT1, sodium-dependent glucose transporter 1; TF, theaflavin; TF3G, theaflavin-3-*O*-gallate; TF3′G, theaflavin-3′-*O*-gallate; TFdG, theaflavin-3,3′-di-*O*-gallate; TJ, tight-junction.

* Corresponding author.
*E-mail address:* tmatsui@agr.kyushu-u.ac.jp (T. Matsui).
[1] These authors contributed equally to this work.

https://doi.org/10.1016/j.jff.2020.104273
Received 25 June 2020; Received in revised form 16 September 2020; Accepted 1 November 2020
Available online 13 November 2020

Martineau, Benhaddou-Andaloussi, Arnason, Lévy, & Pierre, 2010; Meddah et al., 2009).

Glucose derived from digestive processes cannot cross the lipidic intestinal cell membrane, requiring the action of specific transporters, such as sodium-dependent glucose transporter 1 (SGLT1) (Dyer, Hosie, & Shirazi-Beechey, 1997) and glucose transporter 2 (GLUT2) (Zheng, Scow, Duenes, & Sarr, 2012). Thus, modulating the activity of these key transporters is expected to result in an effective physiological amelioration of hyperglycemia. Phlorizin (Ehrenkranz, Lewis, Kahn, & Roth, 2005), a flavonoid glycoside, is a known competitive inhibitor of SGLT1, while its aglycone, phloretin (Behzad et al., 2017), is involved in the GLUT2 glucose transport route. Alzaid, Cheung, Preedy, and Sharp (2013) reported that short-term exposure of Caco-2 cells to an anthocyanin-rich berry extract resulted in a significant reduction in glucose transport via both the SGLT1 and GLUT2 routes, while long-term exposure suppressed glucose transport only via the GLUT2 transport route. During the course of our studies on intestinal absorption of food compounds (Li et al., 2018; Matsui, 2015), theaflavins, typical catechin dimers bearing a characteristic 7-membered ring structure (or benzotropolone skeleton), were found to be incapable of penetrating or crossing the intestinal membrane (Park, Kunitake, & Matsui, 2013). By matrix-assisted laser desorption/ionization mass spectrometry (MALDI-MS) imaging (Nguyen et al., 2019), it has been demonstrated visually that the non-absorbable theaflavins were being incorporated into rat intestinal cells through both the monocarboxylic transporter (MCT) and the organic anion-transporting polypeptides (OATPs), and subsequently effluxed back into the gut via ATP-binding cassette (ABC) transporters. During the transport process of theaflavins, intracellular AMP-dependent kinase (AMPK) was activated in Caco-2 cells, which suppresses the expression of the PepT1 transporter (Takeda, Park, Kunitake, Yoshiura, & Matsui, 2013) and fortifies the membrane barrier by closing the tight-junction (TJ) route (Park, Kunitake, Hirasaki, Tanaka, & Matsui, 2015). It has been reported that a close relationship exists between AMPK phosphorylation (p-AMPK) and the downregulation of SGLT1 mRNA in Caco-2 cells (Sopjani et al., 2010), and that theaflavins exhibit an anti-hyperglycemic effect by attenuating type 1 diabetes-induced intestinal $Na^+/K^+$-ATPase disturbance (Qu et al., 2019); however, studies on the regulation of intestinal glucose transport or transporters by theaflavins have not been conducted. Thus, in this study, the effect of theaflavins on glucose transport across Caco-2 cell monolayers and the underlying mechanisms were investigated.

## 2. Material and methods

### 2.1. Materials

Caco-2 cells were obtained from the research institution of RIKEN Bio-Resource Center (RCB0988, Lot: 53, RIKEN NRC, Tsukuba, Japan). Theaflavin (TF) (201–15161, Lot: WDE1540), TF-3-*O*-gallate (TF3G) (202-15191, Lot: PTR2501), TF-3′-*O*-gallate (TF3′G) (NH030301, Lot: 0020) and TF-3,3′-di-*O*-gallate (TFdG) (208-15171, Lot: PTQ2878) were purchased from Wako Pure Chemical Ind. (Osaka, Japan). Purpurogallin was purchased from Pfaltz & Bauer Inc. (c29590093, Lot: 51932; Waterbury, CT, USA). Dulbecco's modified Eagle's medium (DMEM) (12800-017, Lot: 2027913) and fetal bovine serum (FBS) (2024-01, Lot: 35010168) were purchased from Gibco Life Technologies (Grand Island, NY, USA). Seeding basal medium, enterocyte differentiation medium (05496, Lot: 9343256), and MITO+$^{TM}$ serum extender (355006, Lot: 40480) were purchased from BD Biosciences (Franklin Lakes, NJ, USA). Non-essential amino acid mixture was purchased from MP Biomedicals (1681049, Lot: C2394; Irvine, CA, USA). Penicillin was purchased from Meiji Seika Co. (00901, Lot: C6PGSD; Tokyo, Japan). Streptomycin was purchased from Nacalai Tesque Co. (32204-92, Lot: M7P6082; Kyoto, Japan). Compound C (171260-5MG, Lot: 2730778), an AMPK inhibitor, was purchased from Merck (Darmstadt, Germany). Cyclosporine A, a non-specific inhibitor of ABC efflux transporters, was purchased from Nacalai Tesque (12281-44, Lot: M9G4481). Estrone-3-sulphate (E9145-100MG, Lot: 126M4024V, a competitive inhibitor of OATP), fluorescein (46960, Lot: 456103/1; a competitive inhibitor of MCT), and dantrolene [D9175, Lot: 061M4013; a specific inhibitor of the endoplasmic reticulum (ER) $Ca^{2+}$-release channel ryanodine receptor, RyR] were purchased from Sigma-Aldrich (St. Louis, MO, USA). 2-Aminoethoxydiphenyl borate [2-APB; BML-CA238, Lot: 3-H2331c; a specific inhibitor of the ER $Ca^{2+}$-release channel inositol 1,4,5-

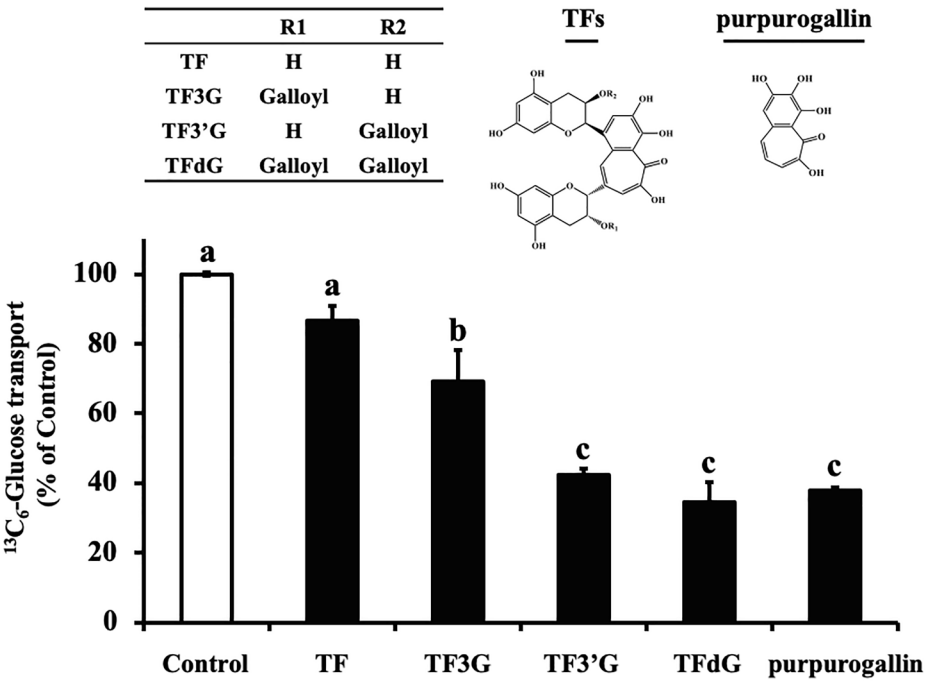


**Fig. 1. Effects of theaflavins on glucose transport across Caco-2 cell monolayers.** Caco-2 cells were treated with 40 μM of each theaflavin and purpurogallin for 24 h. Transport experiments and PMP-derivatization of $^{13}C_6$-glucose were performed as described in section 2.3. Results are expressed as the mean ± SEM ($n = 3$). Statistical differences among the groups were evaluated by the Tukey-Kramer's *t*-test. The different letters represent statistical differences at $p < 0.05$.

triphosphate receptor, $IP_3R$] was purchased from Enzo Life Sciences, Inc. (Burlington, Ontario, Canada). STO-609, a selective inhibitor of $Ca^{2+}$/calmodulin-dependent protein kinase (CaMKK) β, was purchased from FOCUS Biomolecules (10-1036, Lot: 2101377; Plymouth Meeting, PA, USA). Fluo 4-AM was purchased from Dojin Glocal Co. Ltd. (4987481586031, Lot: PH530; Kumamoto, Japan). $^{13}C_6$-Glucose was purchased from Cambridge Isotope Laboratories, Inc. (CLM-1396-1, Lot: PR-23964; Andover, MA, USA). Other regents were of analytical grade and were used without further purification.

### 2.2. Cell culture

Caco-2 cells were cultured in DMEM containing 10% FBS, 100 U/mL of penicillin and 100 μg/L streptomycin. The cells were incubated at 37 °C in humidified atmosphere (5% $CO_2$ and 95% $O_2$), and the medium was exchanged in every alternative day until the cells reached 80–90% confluence, generally within 5–7 days. Caco-2 cells used in this study were between passages of 50 and 60.

For the transport study, cell culture conditions were maintained as described previously (Li et al., 2018). Briefly, Caco-2 cells at a density of $4 \times 10^5$ cells/mL were seeded into a BD Falcon cell culture insert (PET membrane, 0.9 $cm^2$, 1.0 μm pore size; BD Bioscience, Tokyo, Japan) coated with type I collagen (collagen gel culturing kit, Cell matrix type I-A; Nitta Gelatin, Osaka, Japan). Seeded cells were cultured in a seeding basal medium containing MITO+™ serum extender for 48 h. The medium was replaced with an enterocyte differentiation medium containing MITO+™ serum extender every day for 3 days to allow the cells to form monolayers. The integrity of the monolayers was evaluated by measuring transepithelial electrical resistance (TEER) using a multi-channel voltage/current EVC-4000 system (World Precision Instruments, Sarasota, FL, USA). Monolayers with TEER values of >400 Ω $cm^2$ were used for transport experiments.

### 2.3. Treatment of Caco-2 cells with theaflavins for glucose transport experiments

Caco-2 cell monolayers on the transwell (BD Falcon cell culture insert) were treated with theaflavins (10, 20, or 40 μM) in DMEM supplemented with 10% FBS for 6, 12, 24, or 48 h at 37 °C. Cells incubated in theaflavin-free medium were used as controls for the $^{13}C_6$-glucose transport study. For the inhibition study, Caco-2 cells were treated with theaflavins in the presence of inhibitor (10 μM compound C, 20 μM cyclosporine A, 100 μM estrone-3-sulphate, or 100 μM fluorescein) for 24 h prior to $^{13}C_6$-glucose transport experiments. Stocked theaflavin solution dissolved in DMSO was diluted with culture medium (final concentration of DMSO was 0.5% to avoid cell damage). All experiments were conducted in triplicate.

$^{13}C_6$-Glucose was used throughout the evaluation of glucose transport across Caco-2 cell monolayers. Briefly, 1 mM $^{13}C_6$-glucose dissolved in HBSS buffer (pH 6.0) was added to the apical side. After 30 min of transport, 300 μL of the solution was taken from the basolateral side, and 50 μL of 100 μM *N*-acetyl-D-glucosamine (005-20, Lot: M8R8141; Nacalai Tesque) as the internal standard (IS) was added to it. Prior to $^{13}C_6$-glucose analysis by liquid chromatography-time-of-flight-mass

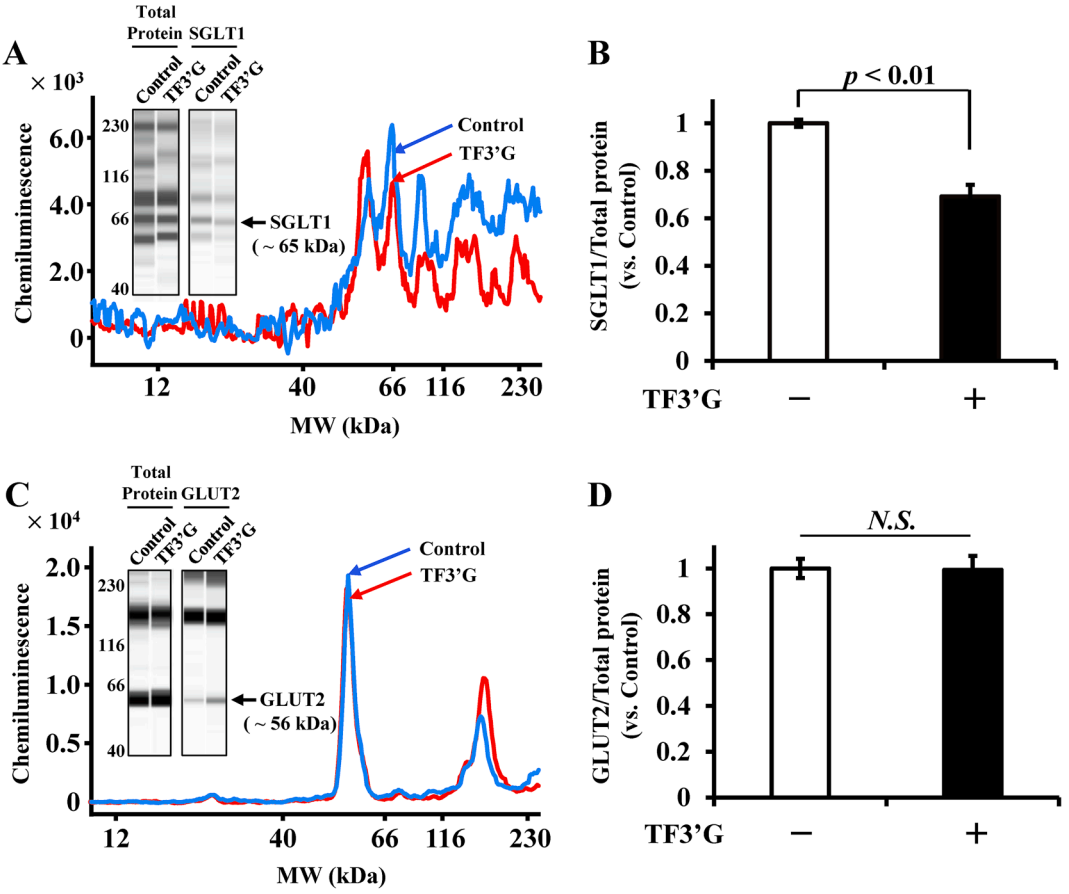


**Fig. 2. Analysis of the effect of TF3′G on the expression of SGLT1 and GLUT2 in Caco-2 cells by Wes analysis.** Caco-2 cells were treated with 40 μM TF3′G for 24 h. Protein levels of SGLT1 (A, B) and GLUT2 (C, D) were measured on a capillary electrophoretic-based immunoassay Wes instrument, as described in section 2.4. The chemiluminescent signal is displayed as a virtual blot-like image, and an electropherogram is generated based on molecular weights. Protein expression of SGLT1 (B) and GLUT2 (D) was normalized by the electropherogram peak area of total protein applied in each lane. Results are expressed as the mean ± SEM ($n = 3$). The statistical difference between the two groups was evaluated by the Student's *t*-test. *N.S.*: no significance at $p < 0.05$.

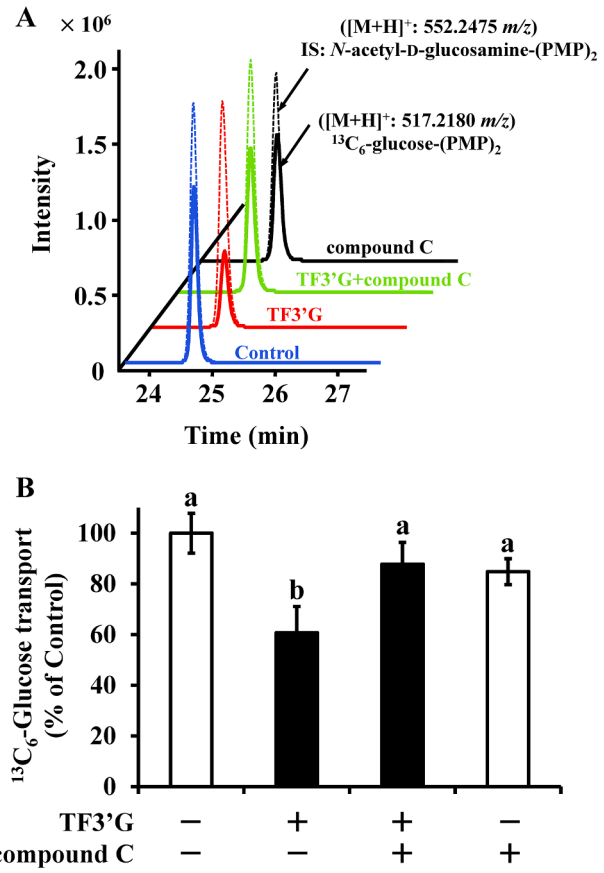


**Fig. 3. Effect of AMPK inhibition on TF3′G-induced inhibition of $^{13}C_6$-glucose transport across Caco-2 cell monolayers.** Typical LC-TOF/MS chromatograms (A) and the transport (B) of $^{13}C_6$-glucose across Caco-2 cell monolayers in the presence and absence of 10 μM compound C (AMPK inhibitor). Caco-2 cells were treated with 40 μM TF3′G for 24 h. Transport experiments and PMP-derivatization of $^{13}C_6$-glucose and *N*-acetyl-D-glucosamine used as IS, were performed as described in section 2.3. Dotted MS chromatograms show IS signals. MS chromatograms in positive ESI mode ($[M + H]^+$) were obtained at 517.2180 *m/z* and 552.2473 *m/z* for PMP-$^{13}C_6$-glucose and PMP-IS, respectively. Results are expressed as the mean ± SEM ($n = 3$). Statistical differences among the groups were evaluated by the Tukey-Kramer's *t*-test. The different letters represent statistical differences at $p < 0.05$.

spectrometry (LC-TOF-MS), derivatization of the mixture solution with 1-phenyl-3-methyl-5-pyrazolone (PMP, M70800-100G, Lot: BCBK6062V; Sigma-Aldrich Co.) was performed as described previously (Li et al., 2018).

LC separation was performed on an Agilent 1200 series HPLC system (Agilent, Waldbronn, Germany), with a Cosmosil 5C18-MS-II column (2.0 mm × 150 mm, Nacalai Tesque) at 40 °C with a linear gradient elution using 0.1% FA (solvent A) and methanol containing 0.1% FA (solvent B) for 20 min at a flow rate of 0.2 mL/min. *N*-Acetyl-D-glucosamine-$(PMP)_2$ ($[M+H]^+$: 552.2473 *m/z*), and $^{13}C_6$-glucose-$(PMP)_2$ ($[M+H]^+$: 517.2180 *m/z*) were analyzed on a micrOTOF II mass spectrometer (Bruker Daltonics, Bremen, Germany). MS conditions in a positive electrospray-ionization (ESI) mode were as follows: dry gas, $N_2$; flow rate, 8.0 L/min; drying gas temperature, 200 °C; drying gas pressure, 1.6 bar; HV capillary voltage, −4500 V; capillary exit, 100.0 V for *N*-acetyl-D-glucosamine-$(PMP)_2$ and $^{13}C_6$-glucose-$(PMP)_2$; hexapole RF, 150 Vpp for *N*-acetyl-D-glucosamine-$(PMP)_2$ and $^{13}C_6$-glucose-$(PMP)_2$; mass range, 100–1500 *m/z*. Data were analyzed using Bruker Data Analysis software, version 3.2.

### 2.4. Quantification of $[Ca^{2+}]_i$ by a fluorescence probe assay and protein expression by a Wes analysis

Intracellular $Ca^{2+}$ concentration ($[Ca^{2+}]_i$) was measured by a Fluo-4 fluorescence probe assay, according to our previous report (Kumrungsee et al., 2014). Shortly, changes in fluorescence intensity, arising from the addition of 40 μM TF3′G to Fluo 4-AM-incorporated Caco-2 cells, were measured at excitation/emission wavelengths of 485 nm/515 nm with a Flex station 2 fluorometer (Molecular Devices, Tokyo, JAPAN). Protein levels of SGLT1, GLUT2, p-AMPK, and AMPK in Caco-2 cells were quantitated on a capillary electrophoretic-based immunoassay Wes instrument (ProteinSimple Co., San Jose, CA, USA). Briefly, Caco-2 cells were treated with theaflavins in the presence of inhibitor (20 μM cyclosporine A, 100 μM estrone-3-sulphate, 100 μM fluorescein, 25 μM STO-609, 100 μM 2-APB, or 50 μM dantrolene) for 24 h at 37 °C. To obtain cell lysates, RIPA buffer containing 0.1% (v/v) Nonidet P-40 (25223-04, Lot: M7B7874; Nacalai Tesque), 1% (v/v) protease inhibitor cocktail (25955-24, Lot: L9T1242; Nacalai Tesque), and PhosSTOP (04906845001, Lot: 41659400; Roche, Indianapolis, IN, USA), were added and the resulting mixture was homogenized with a Polytron homogenizer (KINEMATICA AG, Luzern, Switzerland) at 20,000 rpm for 30 s at 4 °C. Following the centrifugation of the homogenate at 16,000 × *g* for 20 min at 4 °C, supernatants were combined with a 0.1 × Sample Diluent buffer (Protein Simple Co.) to obtain 2.0 μg/μL (for SGLT1 assay) or 0.5 μg/μL (for GLUT2, p-AMPK, and AMPK assays) protein concentration. Four volumes of the diluted samples were mixed with one volume of 5 × Fluorescent Master Mix containing 5% SDS and 200 mM dithiothreitol, followed by the denaturation at 95 °C for 5 min.

The Wes measurement was operated using a 12–230 kDa Separation Module (8 × 25 mm capillary cartridge, ProteinSimple Co.), according to the protocol from our previous report (Tanaka et al., 2020) with several modifications. Wes reagents (biotinylated ladder and primary antibodies) were dispensed in a microplate and subjected to a Wes automated capillary electrophoresis, followed by an automated immune-detection using a horseradish peroxidase-conjugated anti-rabbit secondary antibody and a chemiluminescent substrate. Primary antibodies against SGLT1 (1:100 dilution, ab14686, Lot: GR161462-6; Abcam, Cambridge, UK), GLUT2 (1:200 dilution, ab192599, Lot: GR3213891-2; Abcam), p-AMPK (1:100 dilution, 07-681, Lot: 2193168; Merck Millipore, Bedford, MA, USA), and AMPK (1:200 dilution, 07-350, Lot: 2922422; Merck Millipore) were used. For total protein detection, a pentafluorophenyl ester-biotin labeling reagent, capable of attachment to the applied proteins, was used. At the end of the run, the chemiluminescent signal was displayed as a virtual blot-like image, and an electropherogram was generated based on molecular weights, using ProteinSimple Compass software. Protein expression of SGLT1, GLUT2, p-AMPK, and AMPK was normalized using the electropherogram peak area of total protein applied in each lane, and the data were expressed as the ratios against control.

### 2.5. Statistical analysis

Results are expressed as the mean ± standard error of the mean (SEM). Statistical differences among groups were evaluated by one-factor analysis of variance (ANOVA), followed by Tukey-Kramer's *t*-test for *post hoc* analysis. Statistical evaluation between two groups was performed by the Student's *t*-test. A *p* value of $<0.05$ was considered as significant. All analyses were conducted with a Stat View J5.0 (SAS Institute Inc., Cary, NC, USA).

## 3. Results

### 3.1. Effect of theaflavins on glucose transport across Caco-2 cell monolayers

As an extension to our previous studies, whereby it was established

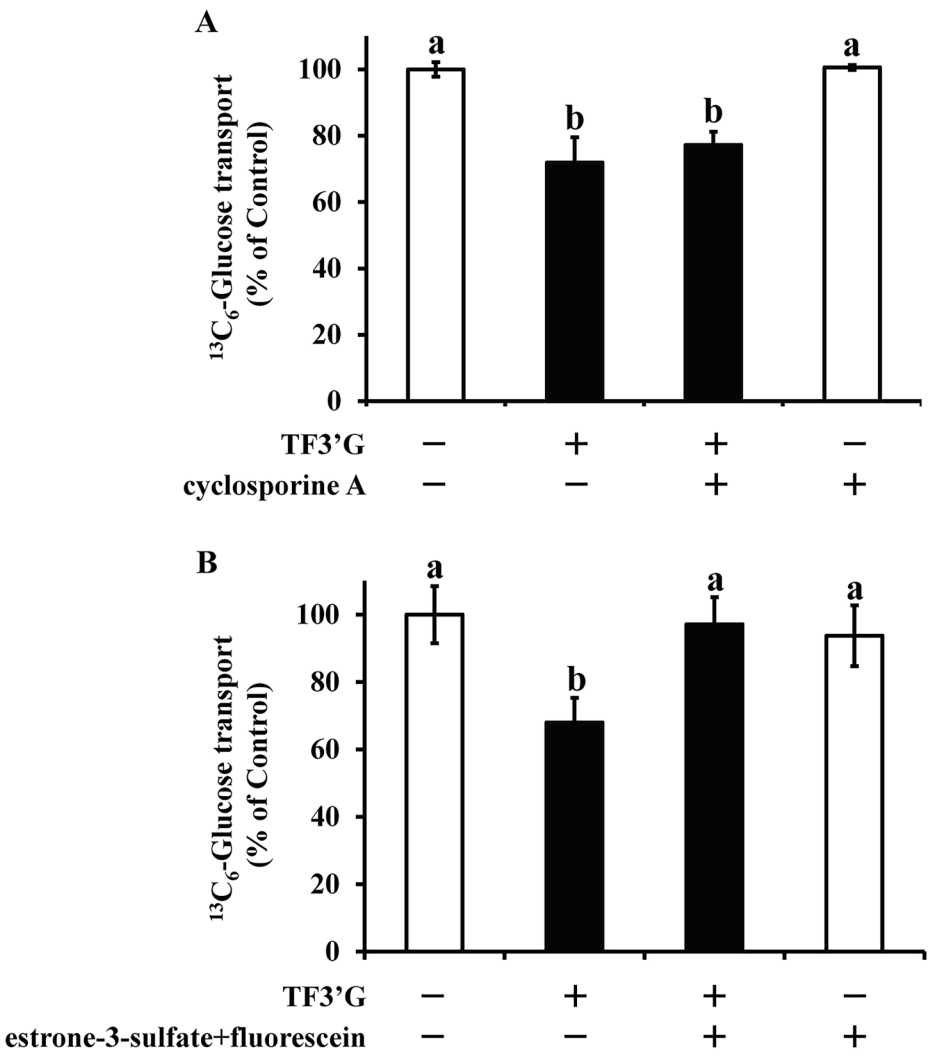


**Fig. 4. Role of efflux/influx routes in TF3′G-induced reduction of $^{13}C_6$-glucose transport across Caco-2 cell monolayers.** $^{13}C_6$-Glucose transport experiments in Caco-2 cell monolayers were performed in the presence and absence of 20 μM cyclosporine A (ABC transporter inhibitor) (A) and 100 μM OATP/MCT inhibitors (estrone-3-sulfate and fluorescein) (B) for 60 min. Caco-2 cells were treated with 40 μM TF3′G for 24 h. Results are expressed as the mean ± SEM ($n$ = 3). Statistical differences among the groups were evaluated by the Tukey-Kramer's $t$-test. The different letters represent statistical differences at $p < 0.05$.

that non-absorbable theaflavins (Matsui, 2015) modulated intestinal transport routes (suppression of PepT1 expression and closure of the TJ via the activation of AMPK during the influx/efflux transport process) (Takeda et al., 2013; Park et al., 2015), the effects of theaflavin treatment (40 μM theaflavins for 24 h) of Caco-2 cell monolayers on $^{13}C_6$-glucose transports was investigated employing TF, TF3G, TF3′G, and TFdG. As seen in Fig. 1, it is evident that all the tested compounds, except for TF, exhibited potential anti-diabetic effects through the inhibition of $^{13}C_6$-glucose transport across Caco-2 cell monolayers. Likewise, purpurogallin displayed a significant ($p < 0.05$) reduction in $^{13}C_6$-glucose transport, indicating that the benzotropolone 7-ring moiety of theaflavins was involved in the inhibitory process. As a significant inhibition of $^{13}C_6$-glucose transport was observed in Caco-2 cells treated with > 20 μM TF3′G for > 24 h (Fig. S1), Caco-2 cells were treated with 40 μM TF3′G for 24 h in further experiments. As we have previously concluded that the benzotropolone moiety of the theaflavins was responsible for AMPK activation in Caco-2 cells (Park et al., 2013), AMPK-related signaling pathways were predominantly targeted in this study to elucidate the mechanism of theaflavin-induced inhibition of intestinal glucose transport.

### 3.2. Effect of TF3′G on the expression of glucose transporters in Caco-2 cells

Expression of the intestinal glucose transport-related transporters SGLT1 and GLUT2 was examined by Wes analysis after Caco-2 cells were treated with 40 μM TF3′G for 24 h. It was evident that TF3′G treatment of Caco-2 cells resulted in a significant ($p < 0.05$) reduction of SGLT1 expression (Fig. 2A-B), whereas GLUT2 expression was not affected by TF3′G (Fig. 2C-D).

### 3.3. Effect of AMPK on TF3′G-induced inhibition of glucose transport across Caco-2 cell monolayers

Based on our previous findings on AMPK activation by theaflavins in Caco-2 cells (Takeda et al., 2013; Park et al., 2015), the relationship between AMPK activation and the observed inhibition of glucose transport by theaflavins was investigated in TF3′G-treated Caco-2 cells. The results depicted in Fig. 3 verify that AMPK activation by TF3′G was responsible for the inhibition of intestinal glucose transport, as compound C (an AMPK inhibitor) reversed the TF3′G-mediated inhibition of glucose transport, increasing the glucose transport to the levels observed in the control ($p < 0.05$). Together with our previous finding on the disappearance of increased p-AMPK/AMPK levels following TF3′G treatment in the presence of compound C by western blot analysis (Park et al., 2015), the present Wes analysis additionally confirmed the significant activation of AMPK arising from the treatment of Caco-2 cells with TF3′G (Fig. S2).

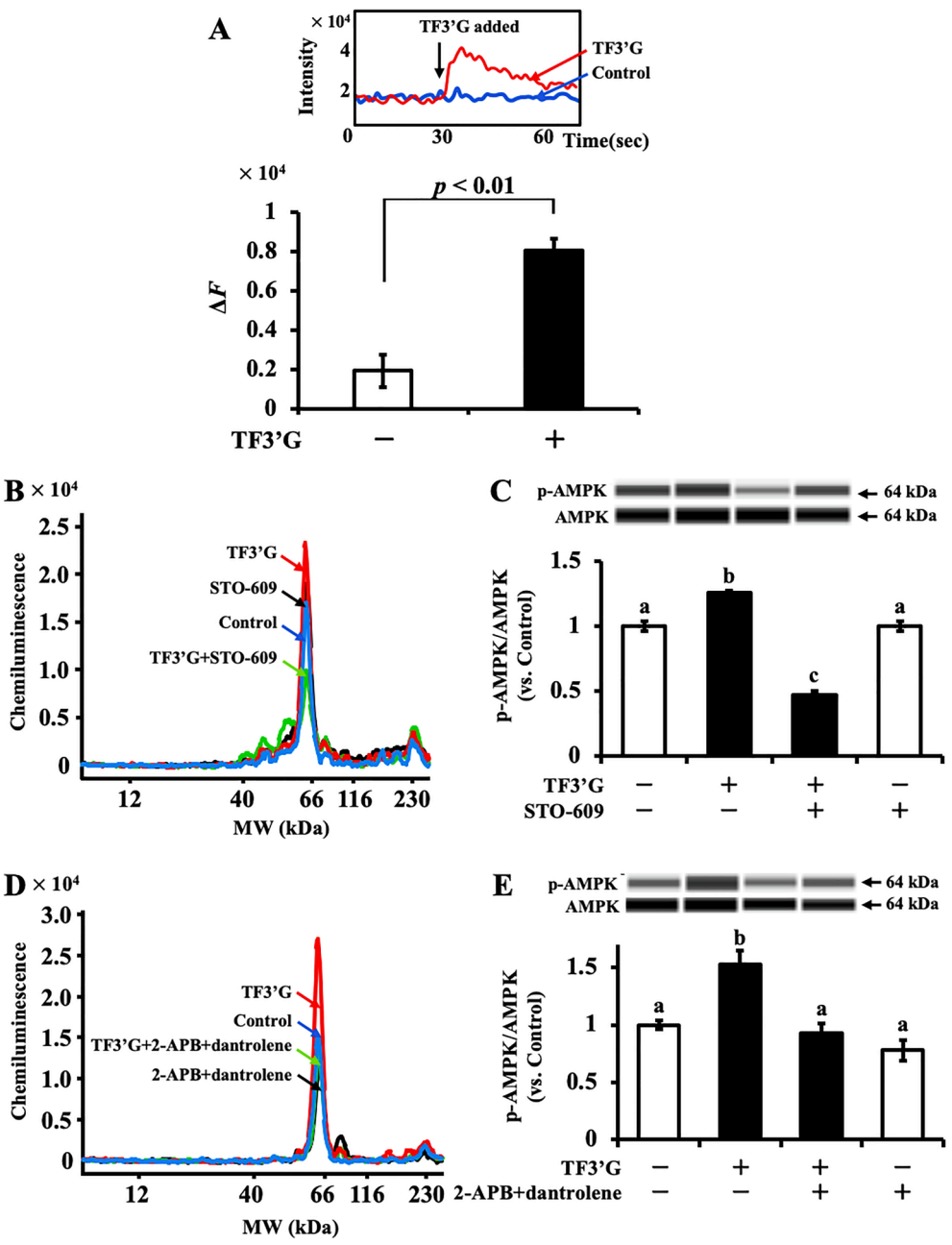


**Fig. 5. Role of $Ca^{2+}$ signaling in TF3′G-induced AMPK activation in Caco-2 cells.** Fluorescence intensity changes resulting from TF3′G effects on $[Ca^{2+}]_i$ were measured by a Fluo-4 fluorescence probe assay at excitation/emission wavelengths of 485 nm/515 nm (A). Protein levels of p-AMPK/AMPK in the presence or absence of 25 μM STO-609 (a selective inhibitor of CaMKK β) (B, C) or in the presence or absence of IP3R/RyR inhibitors (100 μM 2-APB and 50 μM dantrolene for $IP_3R$ and RyR, respectively) (D, E) were measured using a capillary electrophoretic-based immunoassay Wes instrument, as described in section 2.4. Caco-2 cells were treated with 40 μM TF3′G for 24 h. The chemiluminescent signal is displayed as a virtual blot-like image, and an electropherogram is generated based on molecular weights. Protein expression of AMPK and p-AMPK were normalized by the electropherogram peak area of total protein applied in each lane. Results of p-AMPK/AMPK ratio are expressed as the mean ± SEM ($n = 3$). Statistical differences between the two groups and among the groups were evaluated by the Student's *t*-test and Tukey-Kramer's *t*-test, respectively. The different letters represent statistical differences at $p < 0.05$.

### *3.4. Involvement of influx/efflux routes in TF3′G-induced AMPK activation in Caco-2 cells*

Our previous study had visually established that non-absorbable theaflavins were incorporated into the intracellular intestinal membrane via the OATP and MCT routes, with subsequent efflux back into the gut via the ABC efflux transporters (Nguyen et al., 2019). Considering that during the efflux process, the ABC transporters hydrolyze ATP to drive the flux of their substrates, AMPK may be activated in response to ATP consumption (Randak & Welsh, 2005), which would lead to a concomitant increase in the AMP/ATP ratio during the efflux process of theaflavins. As shown in Fig. 4A, the blockage of ABC efflux routes by cyclosporine A did not significantly ameliorate glucose transport inhibition or the elevated p-AMPK expression caused by TF3′G (Fig. S2), suggesting that the efflux events were not involved in TF3′G-induced AMPK activation and glucose transport inhibition across Caco-2 cell monolayers. In contrast, the blocking of possible TF3′G incorporation routes into Caco-2 cells, i.e., the OATP and MCT routes, by both estrone-3-sulfate (Sai et al., 2006) and fluorescein (Konishi, Kobayashi, & Shimizu, 2003), significantly ($p < 0.05$) restored the TF3′G-induced inhibition of glucose transport (Fig. 4B). These results suggested that the influx transport process, or incorporation of TF3′G into the cells, was possibly involved in the AMPK activation. Considering that the intracellular $Ca^{2+}$/CaMKK β signaling cascade involves AMPK activation (Green, Anderson, & Means, 2011), the effects of theaflavins on $[Ca^{2+}]_i$ in Caco-2 cells were investigated. The results from a Fluo-4-fluorescence probe assay (Fig. 5A) indicated that TF3′G significantly ($p < 0.01$) increased the $[Ca^{2+}]_i$, suggesting that TF3′G is a stimulator of $[Ca^{2+}]_i$. Thus, we targeted intracellular $Ca^{2+}$/CaMKK β signaling for AMPK activation, in which the release of $Ca^{2+}$ from the intracellular $Ca^{2+}$ store, the ER, is promoted via the stimulation of $IP_3R$ and RyR receptors in Caco-2 cells (Carrasco-Pozo et al., 2012). As shown in Fig. 5B and 5C, TF3′G-induced activation of AMPK was significantly ($p < 0.05$) abolished by STO-609, a CaMKK β inhibitor, and the abolishment of AMPK

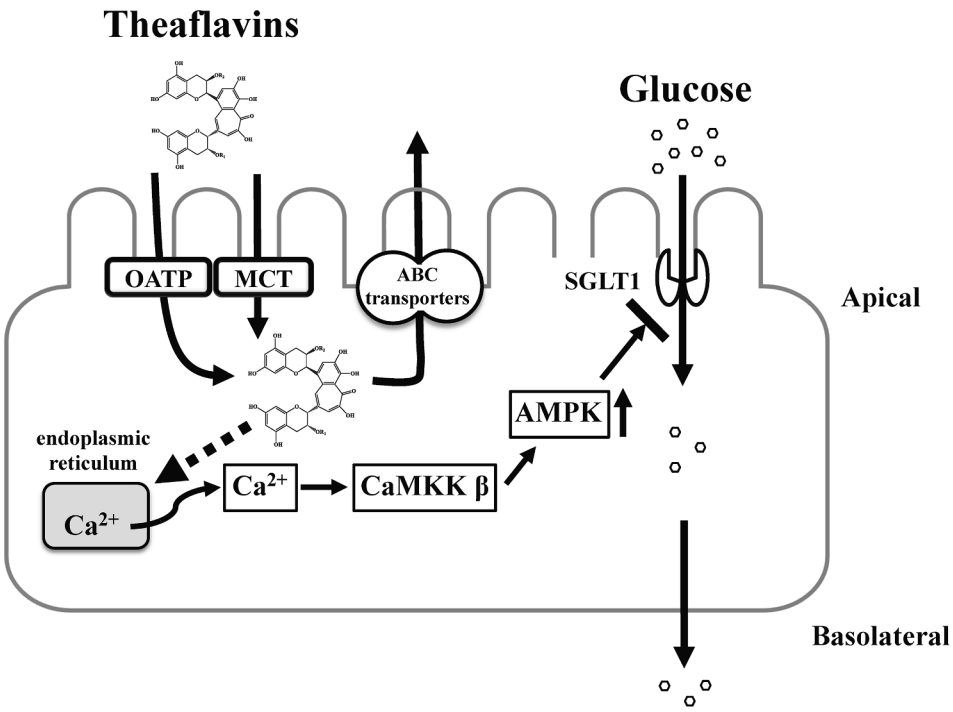


**Fig. 6.** Proposed mechanism underlying the action of non-absorbable theaflavins on glucose transport-related signaling pathways in Caco-2 cells.

activation was likewise observed with $IP_3R$ and RyR inhibitions (Fig. 5D, E). Taken together, these results indicate that either the influx process of TF3′G, or intracellular TF3′G in Caco-2 cells, or both may be involved in the activation of the intracellular $Ca^{2+}$-CaMKK β/AMPK signaling pathway towards SGLT1 suppression.

## 4. Discussion

In this study, treatment of Caco-2 cells with non-absorbable theaflavins caused a significant inhibition of $^{13}C_6$-glucose transport (Fig. 1), suggesting the potential anti-diabetic applicability of theaflavins. In our previous studies, we established that theaflavins inhibited intestinal peptide transport (Takeda et al., 2013) and enhanced intestinal membrane barrier function (Park et al., 2015) by AMPK activation (Park et al., 2013). However, studies on the effects of theaflavins on intestinal glucose transport have not been conducted, although natural phytochemicals, such as quercetin, myricetin (Song et al., 2002), quercetin-3-*O*-rhamnoside (Manzano & Williamson, 2010), and catechins (Kobayashi et al., 2000) inhibited glucose transport. It seems that a benzotropolone 7-ring of theaflavins may be responsible for the effect (Fig. 1), but further studies on structure–activity (reduced glucose transport) relationship (SAR) of polyphenols using monomeric and dimeric catechins, including theaflavins and theasinensins, need to be conducted. In addition, pH stability or degradation of theaflavins during the Caco-2 cell treatment must be also considered for the action, since TF and TF3G showing less effect (Fig. 1) were reported to be unstable at pH 7.4 rather than TF3′G and TFdG (Su, Leung, & Chen, 2003).

Considering previous findings that activated AMPK affected the expression of intestinal transport-related proteins such as PepT1 (Takeda et al., 2013) and TJ-related proteins (Park et al., 2015), and mRNA SGLT1 (Sopjani et al., 2010), the effects of theaflavins on glucose transport-related proteins in Caco-2 cells was examined by a capillary electrophoresis immunoassay-based Wes analysis. It was evident that treatment of Caco-2 cells with 40 μM TF3′G resulted in the restrictive suppression of SGLT1 expression (Fig. 2), uncovering a possible role of theaflavins in reduced glucose transport. SGLT1 expression in oocytes has been shown to be suppressed by natural polyphenols such as quercetin and quercetin-4′-*O*-glucoside (Johnston, Sharp, Clifford, & Morgan, 2005), whereas tomatoside A (Li et al., 2018), quercetin-3-*O*-rhammnoside, and 5-*O*-caffeoylquinic acid (Williamson, 2013) favorably suppressed GLUT2 expression. The characteristic behavior of polyphenols whereby they suppress the expression of glucose transporters may be due to their ability to stimulate the AMPK/SGLT1 (Sopjani et al., 2010), PKCs/GLUT2 (Li et al., 2020; Williamson, 2013), or other cascades, including the $Na^+$, $K^+$-ATPase/SGLT1 cascade (Qu et al., 2019). In addition, considering that CaMKK β activation may cause not only AMPK phosphorylation (Fig. 5C), but also membrane protein phosphorylation (or membrane potential) such as $Ca^{2+}$ and $K^+$ channels (Byun et al., 2012; Kobayashi, Fukuda, Tanaka, & Matsui, 2012), CaMKK β/membrane potential/SGLT1 translocation to membrane cascade might be involved in the theaflavin-induced SGLT1 suppression (Fig. 2A, B). Thus, the relationship between polyphenol structure and signaling cascades towards the suppression of glucose transporters requires extensive investigation in future studies.

In a previous report, we visually demonstrated that the theaflavin TF3′G incorporated into the rat jejunum membrane via the OATP/MCT routes was pumped out into the gut via ABC transport routes (Nguyen et al., 2019). Although the involvement of the efflux process of theaflavins in the AMPK activation can be excluded by the present study's results (Fig. 4A and Fig. S2), it remains unascertained whether the OATP/MCT influx process or intracellular theaflavin in Caco-2 cells are responsible for the activated AMPK-induced suppression of SGLT1 expression. The report that a cyclooxygenase inhibitor, indometacin (Carrasco-Pozo et al., 2012), enhanced intracellular $Ca^{2+}$ release from the ER through the activation of $IP_3R$ and RyR allows the speculation that "intracellular" theaflavins, which can increase the $[Ca^{2+}]_i$ (Fig. 5A), may be involved in the elevation of ER-$Ca^{2+}$ release/activation of CaMKK β (Fig. 5C, E). However, according to our previous finding that a non-absorbable steroidal saponin, tomatoside A, was incorporated via the apical sodium-dependent bile acid transporter (ASBT) to activate PKCs, but not AMPK, in Caco-2 cells (Li et al., 2018), influx routes may also determine signaling cascades related to glucose transporter expression. Direct evidence on the involvement of influx routes or intracellular non-absorbable molecules in the above signaling activation must be provided in future studies by various techniques, for e.g., *in silico* quantum mechanical analysis of theaflavins with targetable

proteins including $IP_3R$, RyR, and their upstream enzymes (Kumrungsee et al., 2014; Cao et al., 2015; Park et al., 2019).

## 5. Conclusions

In conclusion, it was demonstrated for the first time that theaflavins, as intestinally non-absorbable compounds, possess the ability to inhibit intestinal glucose transport across Caco-2 cell monolayers. The action of theaflavins resulted from the suppression of SGLT1 partly via CaMKK β/AMPK activation, but not GLUT2 expression. Taken together, non-absorbable theaflavins may be useful as anti-hyperglycemic functional food compounds for the prevention of diabetes via ER-$Ca^{2+}$/CaMKK β/AMPK activation (Fig. 6).

## Ethics statement

The authors have declared that no animal experiments exist in this study.

## Author Statement

Baorui Li, Lei Fu, Chizumi Abe, Alexia M. Nectoux, and Ayaka Yamamoto performed experiments and analyzed data; Baorui Li, Lei Fu, and Toshiro Matsui wrote the manuscript. Toshiro Matsui designed the study, interpreted, analyzed data, and reviewed and edited the manuscript.

## Declaration of Competing Interest

This research did not receive any specific grant from funding agencies in the public, commercial, or not-for-profit sectors.

## Acknowledgments

This work was supported by JSPS KAKENHI Grant Number JP18H02157 to T.M.

## Appendix A. Supplementary material

Supplementary data to this article can be found online at https://doi.org/10.1016/j.jff.2020.104273.

## References

Abesundara, K. J., Matsui, T., & Matsumoto, K. (2004). α-Glucosidase inhibitory activity of some Sri Lanka plant extracts, one of which, *Cassia auriculata*, exerts a strong antihyperglycemic effect in rats comparable to the therapeutic drug acarbose. *Journal of Agricultural and Food Chemistry, 52*(9), 2541–2545.

Alzaid, F., Cheung, H. M., Preedy, V. R., & Sharp, P. A. (2013). Regulation of glucose transporter expression in human intestinal Caco-2 cells following exposure to an anthocyanin-rich berry extract. *PLoS One, 8*(11), Article e78932.

Baldea, L. A. N., Martineau, L. C., Benhaddou-Andaloussi, A., Arnason, J. T., Lévy, É., & Haddad, P. S. (2010). Inhibition of intestinal glucose absorption by anti-diabetic medicinal plants derived from the James Bay Cree traditional pharmacopeia. *Journal of Ethnopharmcology, 132*(2), 473–482.

Behzad, S., Sureda, A., Barreca, D., Nabavi, S. F., Rastrelli, L., & Nabavi, S. M. (2017). Health effects of phloretin: From chemistry to medicine. *Phytochemistry Reviews, 16*(3), 527–533.

Byun, E. B., Korematsu, S., Ishikawa, T., Nishizuka, T., Ohshima, S., Kanda, T., & Matsui, T. (2012). Apple procyanidins induce hyperpolarization of rat aorta endothelial cells via activation of $K^+$ channels. *Journal of Nutritional Biochemistry, 23*(3), 278–286.

Cao, R., Kobayashi, Y., Nonaka, A., Miyata, Y., Tanaka, K., Tanaka, T., & Matsui, T. (2015). NMR spectroscopic and quantum mechanical analyses of enhanced solubilization of hesperidin by theasinensin A. *Pharmaceutical Research, 32*(7), 2301–2309.

Carrasco-Pozo, C., Pastenec, E., Vergarae, C., Zapatae, M., Sandovald, C., & Gotteland, M. (2012). Stimulation of cytosolic and mitochondrial calcium mobilization by indomethacin in Caco-2 cells: Modulation by the polyphenols quercetin, resveratrol and rutin. *Biochimica et Biophysica Acta-Gene Subjects, 1820*(12), 2052–2061.

Dyer, J., Hosie, K. B., & Shirazi-Beechey, S. P. (1997). Nutrient regulation of human intestinal sugar transporter (SGLT1) expression. *Gut, 41*(1), 56–59.

Ehrenkranz, J. R., Lewis, N. G., Kahn, C. R., & Roth, J. (2005). Phlorizin: A review. *Diabetes/Metabolism Research and Reviews, 21*(1), 31–38.

Green, M. F., Anderson, K. A., & Means, A. R. (2011). Characterization of the CaMKK β–AMPK signaling complex. *Cellular Signalling, 23*(12), 2005–2012.

Hu, F. B. (2011). Globalization of diabetes: The role of diet, lifestyle, and genes. *Diabetes Care, 34*(6), 1249–1257.

Johnston, K., Sharp, P., Clifford, M., & Morgan, L. (2005). Dietary polyphenols decrease glucose uptake by human intestinal Caco-2 cells. *FEBS Letters, 579*(7), 1653–1657.

Kobayashi, Y., Fukuda, T., Tanaka, M., & Matsui, T. (2012). The anti-atherosclerotic dipeptide, Trp-His, inhibits the phosphorylation of voltage-dependent L-type $Ca^{2+}$ channels in rat vascular smooth muscle cells. *FEBS Open Bio, 2*, 83–88.

Kobayashi, Y., Suzuki, M., Satsu, H., Arai, S., Hara, Y., Suzuki, M., … Shimizu, M. (2000). Green tea polyphenols inhibit the sodium-dependent glucose transporter of intestinal epithelial cells by a competitive mechanism. *Journal of Agricultural and Food Chemistry, 48*(11), 5618–5623.

Konishi, Y., Kobayashi, S., & Shimizu, M. (2003). Tea polyphenols inhibit the transport of dietary phenolic acids mediated by the monocarboxylic acid transporter (MCT) in intestinal Caco-2 cell monolayers. *Journal of Agricultural and Food Chemistry, 51*(25), 7296–7302.

Kumrungsee, T., Saiki, T., Akiyama, S., Nakashima, K., Tanaka, M., Kobayashi, Y., & Matsui, T. (2014). Inhibition of calcium-calmodulin complex formation by vasorelaxant basic dipeptides demonstrated by *in vitro* and *in silico* analyses. *Biochimica et Biophysica Acta-General Subjects, 1840*(10), 3073–3078.

Li, B., Terazono, Y., Hirasaki, N., Tatemichi, Y., Kinoshita, E., Obata, A., & Matsui, T. (2018). Inhibition of glucose transport by tomatoside A, a tomato seed steroidal saponin, through the suppression of GLUT2 expression in Caco-2 cells. *Journal of Agricultural and Food Chemistry, 66*(6), 1428–1434.

Li, Q., Wang, C., Liu, F., Hu, T., Shen, W., Li, E., … Zou, Y. (2020). Mulberry leaf polyphenols attenuated postprandial glucose absorption via inhibition of disaccharidases activity and glucose transport in Caco-2 cells. *Food & Function, 11*(2), 1835–1844.

Manzano, S., & Williamson, G. (2010). Polyphenols and phenolic acids from strawberry and apple decrease glucose uptake and transport by human intestinal Caco-2 cells. *Molecular Nutrition & Food Research, 54*(12), 1773–1780.

Matsui, T. (2015). Condensed catechins and their potential health-benefits. *European Journal of Pharmacology, 765*, 495–502.

Matsui, T., Tanaka, T., Tamura, S., Toshima, A., Tamaya, K., Miyata, Y., … Matsumoto, K. (2007). α-Glucosidase inhibitory profile of catechins and theaflavins. *Journal of Agricultural and Food Chemistry, 55*(1), 99–105.

Matsui, T., Ueda, T., Oki, T., Sugita, K., Terahara, N., & Matsumoto, K. (2001). α-Glucosidase inhibitory action of natural acylated anthocyanins. 1. Survey of natural pigments with potent inhibitory activity. *Journal of Agricultural and Food Chemistry, 49*(4), 1948–1951.

Matsumoto, N., Ishigaki, F., Ishigaki, A., Iwashina, H., & Hara, Y. (1993). Reduction of blood glucose levels by tea catechin. *Bioscience, Biotechnology, and Biochemistry, 57*(4), 525–527.

Meddah, B., Ducroc, R., Faouzi, M. E. A., Eto, B., Mahraoui, L., Benhaddou-Andaloussiad, A., … Haddad, P. S. (2009). Nigella sativa inhibits intestinal glucose absorption and improves glucose tolerance in rats. *Journal of Ethnopharmcology, 121*(3), 419–424.

Nguyen, H. N., Tanaka, M., Li, B., Ueno, T., Matsuda, H., & Matsui, T. (2019). Novel in situ visualisation of rat intestinal absorption of polyphenols via matrix-assisted laser desorption/ionisation mass spectrometry imaging. *Scientific Reports, 9*(1), 3166–3175.

Park, H. Y., Kunitake, Y., & Matsui, T. (2013). Benzotropolone moiety in theaflavins is responsible for inhibiting peptide-transport and activating AMP-activated protein kinase in Caco-2 cells. *Functional Foods in Health and Disease, 3*(5), 111–121.

Park, H. Y., Kunitake, Y., Hirasaki, N., Tanaka, M., & Matsui, T. (2015). Theaflavins enhance intestinal barrier of Caco-2 cell monolayers through the expression of AMP-activated protein kinase-mediated occludin, claudin-1, and ZO-1. *Bioscience, Biotechnology, and Biochemistry, 79*(1), 130–137.

Park, J., Selvam, B., Sanematsu, K., Shigemura, N., Shukla, D., & Procko, E. (2019). Structural architecture of a dimeric class C GPCR based on co-trafficking of sweet taste receptor subunits. *Journal of Biological Chemistry, 294*(13), 4759–4774.

Qu, F., Liu, S., He, C., Zhou, J., Zhang, S., Zeyi, A., … Ni, D. (2019). Comparison of the effects of green and black tea extracts on $Na^+/K^+$-ATPase activity in intestine of type 1 and type 2 diabetic mice. *Molecular Nutrition & Food Research, 63*(17), 1801039.

Randak, C. O., & Welsh, M. J. (2005). Adenylate kinase activity in ABC transporters. *Journal of Biological Chemistry, 280*(41), 34385–34388.

Sai, Y., Kaneko, Y., Ito, S., Mitsuoka, K., Kato, Y., Tamai, I., … Tsuji, A. (2006). Predominant contribution of organic anion transport in polypeptide oatp2b1 to apical uptake of estrone-3-sulfate by human intestinal Caco-2 cells. *Drug Metabolism and Disposition, 34*(8), 1423–1431.

Song, J., Kwon, O., Chen, S., Daruwala, R., Eck, P., Park, J. B., & Levine, M. (2002). Flavonoid inhibition of sodium-dependent vitamin C transporter 1 (SVCT1) and glucose transporter isoform 2 (GLUT2), intestinal transporters for vitamin C and glucose. *Journal of Biological Chemistry, 277*(18), 15252–15260.

Sopjani, M., Bhavsar, S. K., Fraser, S., Kemp, B. E., Föller, M., & Lang, F. (2010). Regulation of $Na^+$-coupled glucose carrier SGLT1 by AMP-activated protein kinase. *Molecular Membrane Biology, 27*, 137–144.

Su, Y. L., Leung, L. K., & Chen, Z. Y. (2003). Stability of tea theaflavins and catechins. *Food Chemistry, 83*, 189–195.

Takeda, J., Park, H. Y., Kunitake, Y., Yoshiura, K., & Matsui, T. (2013). Theaflavins, dimeric catechins, inhibit peptide transport across Caco-2 cell monolayers via down-regulation of AMP-activated protein kinase-mediated peptide transporter PEPT1. *Food Chemistry, 138*(4), 2140–2145.

Tanaka, M., Kiyohara, H., Yoshino, A., Nakano, A., Takata, F., Dohgu, S., … Matsui, T. (2020). Brain-transportable soy dipeptide, Tyr-Pro, attenuates amyloid β peptide$_{25-35}$-induced memory impairment in mice. *npj Science of Food, 4*(1), 1–4.

Wilmot, E. G., Edwardson, C. L., Achana, F. A., Davies, M. J., Gorely, T., Gray, L. J., … Biddle, S. J. H. (2012). Sedentary time in adults and the association with diabetes, cardiovascular disease and death: Systematic review and meta-analysis. *Diabetologia, 55*, 2895–2905.

Williamson, G. (2013). Possible effects of dietary polyphenols on sugar absorption and digestion. *Molecular Nutrition & Food Research, 57*(1), 48–57.

Zheng, Y., Scow, J. S., Duenes, J. A., & Sarr, M. G. (2012). Mechanisms of glucose uptake in intestinal cell lines: Role of GLUT2. *Surgery, 151*(1), 13–25.